ACS APPLIED MATERIALS & INTERFACES

Research Article

www.acsami.org

Novel Highly Selective and Reversible Chemosensors Based on Dual-Ratiometric Fluorescent Electrospun Nanofibers with pH- and Fe^{3+}-Modulated Multicolor Fluorescence Emission

Bo-Yu Chen, Chi-Ching Kuo,* Yun-Shao Huang, Shih-Tung Lu, Fang-Cheng Liang, and Dai-Hua Jiang

Institute of Organic and Polymeric Materials, National Taipei University of Technology, 10608 Taipei, Taiwan

Supporting Information

ABSTRACT: Novel dual-ratiometric fluorescent electrospun (ES) nanofibers featuring high sensitivity for pH and ferric ion (Fe^{3+}) were prepared using binary blends of poly(2-hydroxyethyl methacrylate-*co*-*N*-methylolacrylamide-*co*-nitrobenzoxadiazolyl derivative) (poly(HEMA-*co*-NMA-*co*-NBD)) and a spirolactam rhodamine derivative (SRhBOH) by employing a single-capillary spinneret. The HEMA, NMA, and NBD moieties were designed to exhibit hydrophilic properties, chemical cross-linking, and fluorescence (fluorescence resonance energy transfer (FRET) donor), respectively. The fluorescence emission of SRhBOH was highly selective for pH and Fe^{3+}; when SRhBOH detected acidic media and Fe^{3+}, the spirocyclic form of SRhBOH, which is nonfluorescent, was transformed into the opened cyclic form and exhibited strong fluorescence emission. The emission colors of ES nanofibers in acidic or Fe^{3+} aqueous solutions changed from green to red because of FRET from NBD (donor) to SRhBOH (acceptor). The off/on switching of the FRET process was modulated by adjusting the SRhBOH blending ratio, pH, and Fe^{3+} concentration. Poly(HEMA-*co*-NMA-*co*-NBD) ES fibers blended with 20% SRhBOH showed high sensitivity in sensing Fe^{3+} and pH because of the substantial 57 nm red shift in emission as well as substantial reversible dual photoluminescence. The prepared FRET-based dual-ratiometric fluorescent ES nanofibrous membranes can be used as "naked eye" sensors and have potential for application in multifunctional environment sensing devices.

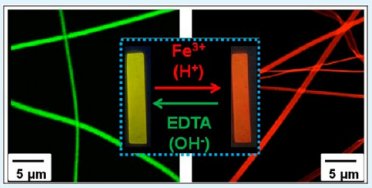

KEYWORDS: *electrospun (ES) nanofibers, luminescence, pH, ferric ion, sensor*

INTRODUCTION

Considerable attention has been focused on selective and sensitive chromogenic or fluorogenic signaling probes for detecting heavy transition metal (HTM) cations and pH because they may cause severe effects on human health and the environment.[1−5] The HTM cations ferric ion (Fe^{3+}) is essential in numerous biological processes.[4−8] For example, it provides the oxygen-carrying capacity of heme and acts as a cofactor in many enzymatic reactions involved in the mitochondrial respiratory chain. In addition, in deficient or excess quantities, Fe^{3+} is toxic and can lead to diseases. In living organisms, pH values exhibit curial effects on cell and tissue activities.[9] Rhodamine B and its derivatives (RhBs) are satisfactory fluorescent probes for sensing various HTM cations including Fe^{3+} and pH because of their unique properties such as a high fluorescence quantum yield, long wavelength emission, high absorption coefficient, favorable photostability, and high sensitivity.[3−5,10−16] Tang reported that RhB chemosensors exhibited substantial turn-on fluorescent and colorimetric response toward Fe^{3+} in aqueous media with high selectivity and sensitivity but exhibited no significant response to other metal ions.[5]

Recently, fluorescence resonance energy transfer (FRET)-based sensors for sensing certain HTM cations and pH have attracted considerable attention because of their simplicity, color variation, and ratiometric detection capability.[17−21] Efficient color tuning can be achieved through FRET from a donor (the wider band gap) to an acceptor (narrower band gap) if the luminescence spectra of the donor overlaps substantially with the absorption spectra of the acceptor. Ma and colleagues reported a FRET-based sensing system for detecting Fe^{3+} in aqueous media that involves using amphiphilic micells containing fluorescent dye, a nitrobenzoxadiazolyl derivative (NBD) (donor), and RhB (acceptor).[20] Liu and colleagues prepared dual-ratiometric fluorescent probes for sensing pH from well-defined copolymers labeled with FRET donor (NBD) and acceptor moieties (RhBs) at the chain middle and terminals.[21] However, all of the aforementioned studies[3−9,14−21] were based on solutions rather than nanofibers. The high surface-to-volume ratio of the nanofibers facilitates responses in Fe^{3+}/pH-sensitive or multifunctional sensory materials.

The electrospinning technique has been used widely in recent studies because it is inexpensive and facile and enables nanometer-scaled fibers to be fine tuned.[22−26] Recently, we prepared various florescent sensory-based electrospun (ES) polymer nanofibers for sensing pH,[27] temperature,[28,29] and NO gas.[30] However, few studies have reported fluorescent ES nanofibers for metal-ion-sensitive optical sensors.[31,32] Samuelson and colleagues reported poly(acrylic acid)-poly(pyrene

Received: November 16, 2014
Accepted: January 14, 2015
Published: January 14, 2015

DOI: 10.1021/am508029x
ACS Appl. Mater. Interfaces 2015, 7, 2797−2808

Scheme 1. Design of Multifunctional Sensory ES Nanofibers from Poly(HEMA-*co*-NMA-*co*-NBD)/SRhBOH Blends with Fluorescence Emission in Various Colors[a]

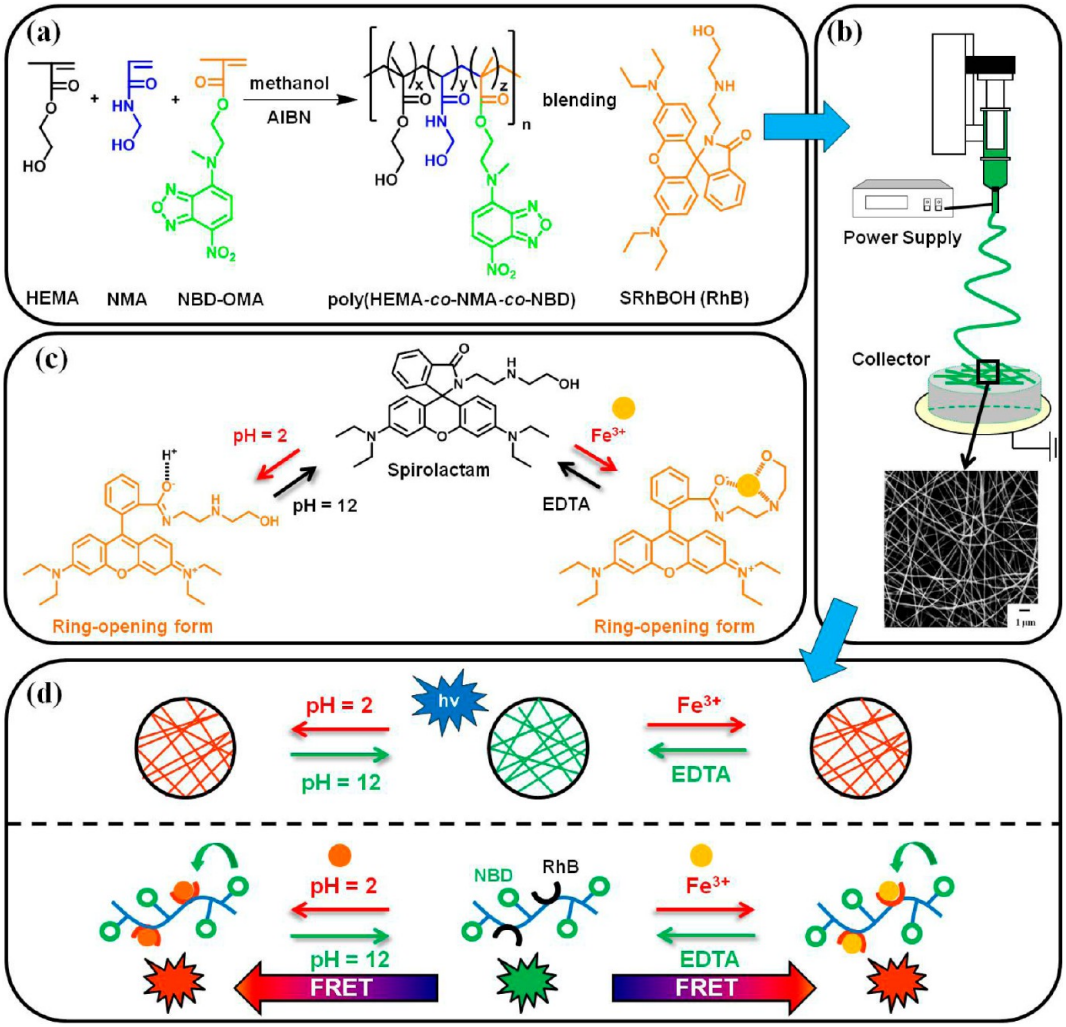

[a](a) Polymerization and chemical structure of poly(HEMA-co-NMA-co-NBD) and SRhBOH. (b) Fabrication of ES nanofibers from the blends. (c) The change in the chemical structure of SRhBOH in solutions with Fe3+ or EDTA or pH 2 or pH 12. (d) The effect of FRET on the change of fluorescent emission colors of multienvironment sensing ES nanofibers.

menthanol) ES nanofibrous membranes that exhibited highly responsive fluorescence quenching-based optical sensors for Fe^{3+} and Hg^{2+}.[31] The novel napthalimide-functionalized ES nanofibrous membranes exhibited high sensitivity in detecting Cu^{2+} in an aqueous solution according to Wang and colleagues.[32] Recently, we collaborated with Meng to develop ES nanofibers from fluorescent probe molecules for Zn^{2+} and hydrogel polymer blends, poly(2-hydroxyethyl methacrylate)-(poly HEMA), to create a real-time Zn^{2+} sensor with high sensitivity and cell medium compatibility.[33] The high surface-to-volume ratio of the ES fibers enhanced their sensitivity compared with that of thin films, as demonstrated by the aforementioned studies.[27−33] Thus, designing a sensing system based on ES florescent nanofibers with tunable Fe^{3+}/pH detection ranges is advantageous.

In this paper, we report new reversible FRET-based chromo- and fluorogenic sensory ES nanofibers that were prepared using synthesized poly(HEMA-*co*-*N*-methylolacrylamide-*co*-NBD) (poly(HEMA-*co*-NMA-*co*-NBD)) copolymers and their blends with a spirolactam rhodamine derivative (SRhBOH) and have dual-Fe^{3+}/pH-sensing characteristics. These multifunctional ES nanofibers comprised poly(HEMA-*co*-NMA-*co*-NBD) containing a hydrogel hydrophilic material (PHEMA), a chemical cross-linkable segment(PNMA), and a fluorescent dye (NBD) moiety, which were blended with a Fe^{3+}-chelating and pH-sensing probe (SRhBOH) by combining synthesis, electrospinning, optical application, and morphological characteristics. The NBD, poly(HEMA-*co*-NMA-*co*-NBD), which was subjected to free-radical polymerization, and SRhBOH were synthesized as shown in Scheme 1a. All copolymers and probes were identified using ^{1}H nuclear magnetic resonance (NMR), electrospray ionization mass spectrometry (ESI-MS), and gel permeation chromatography (GPC). A single-capillary spinneret was used in fabricating ES nanofibers from poly(HEMA-*co*-NMA-*co*-NBD) blended with 1%, 5%, 10%, and 20% SRhBOH; the nanofibers were then post-treated through chemical cross-linking to enhance their stability in water, as shown in Scheme 1b. The morphologies of the ES nanofibers were identified using a field-emission scanning electron microscope (FE-SEM), transmission electron microscope (TEM), and laser confocal microscope. Scheme 1c and 1d shows that the ES nanofiber sensor exhibited reversible dual-fluorogenic switching from

DOI: 10.1021/am508029x
ACS Appl. Mater. Interfaces 2015, 7, 2797−2808

green to red. The fluorescence emission of SRhBOH is highly selective for Fe^{3+} and is pH dependent; when SRhBOH was used to detect Fe^{3+}/acidic media, the spirocyclic form of SRhBOH, which is colorless and nonfluorescent, transformed into the opened cyclic form, which is pink and exhibits strong fluorescent emission (Scheme 1c).[34] The emission of the ES nanofibers changed from green to red because of the energy transfer from NBD (donor) to SRhBOH (acceptor) (Scheme 1d). Thus, the off/on switching of the FRET process can be facilely modulated by adjusting the concentrations of Fe^{3+} or pH. We studied the fluorescent emission transition of various metal ions and their responsiveness in photoluminescence (PL) and ultraviolet−visible (UV−vis) spectra. The favorable reversible detection of Fe^{3+}/pH shown by the experimental results suggested that ES nanofibrous membranes, which can be used as "naked eye" sensors, have potential applications in multifunctional environmental sensing devices.

EXPERIMENTAL SECTION

Materials. HEMA was purchased from Aldrich, purified by passing it through a short aluminum oxide column (50−200 μm), and stored at 4 °C prior to use. NMA was purchased from Tokyo Chemical Industry Co., Japan. In addition, 2,2′-azobis(2-methylpropionitrile) (AIBN) was purchased from UniRegion Bio-Tech and recrystallized two times in ethanol prior to use. RhB (Acros, GR (Guaranteed Reagent)), *N*-(2-hydroxyethyl)ethylenediamine (Aldrich, 99%), 4-chloro-7-nitrobenzofurazan (NBD-Cl, Alfa Aesar, 99%), the Trizma base (Sigma, 99.9%), 2-(methylamino)ethanol (Alfa Aesar, 99%), and methacryloyl chloride (Alfa Aesar, 97%) were used as received. Tetrahydrofuran (THF, Tedia, 99.9%), acetonitrile anhydrous (Tedia, 99%), methanol (Tedia, HPLC/SPECTRO), dichloromethane (Tedia, 99.9%), and ethanol (Sigma-Aldrich, 99.8%) were used as received. The perchlorate salts of metal ions (Co^{2+}, Mg^{2+}, Na^{+}, Cu^{2+}, Fe^{2+}, Fe^{3+}, Pb^{2+}, Zn^{2+}, Cd^{2+}, K^{+}, Ni^{2+}) were purchased from Aldrich. Ethylenediaminetetraacetic acid tetrasodium salt hydrate (EDTA, 98%) was purchased from Alfa Aesar.

Synthesis of a Fluorescent Probe (NBD-OH). The fluorescent NBD (NBD-OMA) was prepared according to a previously reported method[35−37] and is shown in Scheme 2a. In a two-necked round-bottomed flask, 1 g (5.011 mmol) of NBD-Cl was dissolved in 40 mL of ethanol and placed in an oil bath. Under vigorous stirring, excess 2-(methylamino)ethanol was added dropwise. The mixture was refluxed at 60 °C, and the stirring was continued for 2 h. The residue was then filtered, washed with cold ethanol, and purified through recrystallization in ethanol. Thus, 2-[methyl(7-nitro-2,1,3-benzoxadiazol-4 yl)-amino]ethanol (NBD-OH) was produced.

Scheme 2. Synthesis of (a) NBD-OMA Fluorescent Monomer (donor) and (b) SRhBOH Fluorescent Probe (acceptor)

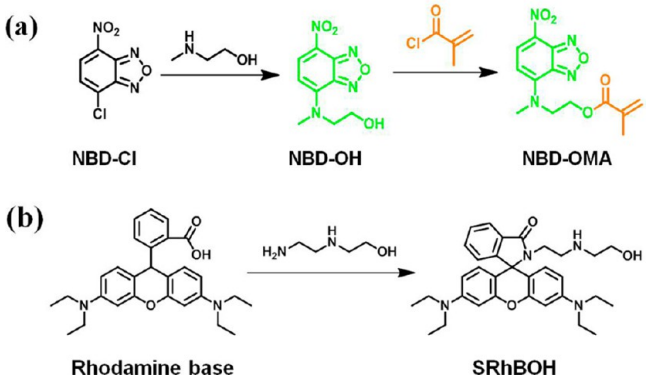

Synthesis of the Fluorescent Monomer (NBD-OMA). In a two-necked round-bottomed flask, 1000 mg (4.2 mmol) of the fluorescent probe, NBD-OH, and excess triethylamine were mixed into THF. The mixture was cooled in an ice water bath. Methacryloyl chloride (2 mL, 21 mmol) was dropped into the stirred solution. The reaction mixture was stirred for 30 h. An ammonium salt precipitated during the reaction. The mixture was filtrated, and the solvent was removed under reduced pressure. The solid was then dissolved in dichloromethane and purified in a silica gel column with dichloromethane/ethyl acetate (100:20) as an eluent. ^{1}H NMR ($CDCl_3$): δ = 8.43 (a, 1H), δ = 6.17 (b, 1H), δ = 5.89 (f, 1H), δ = 5.49 (f, 1H), δ = 4.49 (d, 4H), δ = 3.46 (c, 3H), δ = 1.79 (e, 3H); the ^{1}H NMR spectrum is shown in Figure S1 (Supporting Information).

Synthesis of a Fluorescent Probe (SRhBOH). The synthesis scheme is shown in Scheme 2b. The fluorescent probe, SRhBOH, was synthesized according to a previously reported method.[20] RhB (2.4 g, 5 mmol) and excess *N*-(2-hydroxyethyl)ethylenediamine were dissolved in 40 mL of methanol. The reaction mixture was refluxed for 20 h, and the fluorescence of the solution disappeared. After cooling to room temperature, the solvent was removed under reduced pressure. CH_2Cl_2 (200 mL) was then added, and the solvent was washed with water several times and dried over anhydrous sodium sulfate. After filtration of the sodium sulfate, the solvent was removed under reduced pressure. The resulting solid was purified on a silica gel column with dichloromethane/methanol (5:1) as an eluent. The chemical structure of SRhBOH was characterized using ^{1}H NMR (Figure S2, Supporting Information) and ESI-MS (Figure S3, Supporting Information). ^{1}H NMR ($CDCl_3$): δ = 6.2−7.88 (aromatic hydrogen, 10H), δ = 3.39 (f, 2H), δ = 3.32 (b, 8H), δ = 3.24 (c, 2H), δ = 2.52 (d, 2H), δ = 2.37 (e, 2H), δ = 1.89 (g, 2H), δ = 1.13 (a, 12H).

Synthesis of Poly(HEMA-*co*-NMA-*co*-NBD). The scheme for synthesizing poly(HEMA-*co*-NMA-*co*-NBD) random copolymers is shown in Scheme 1a. In a two-necked round-bottomed flask, 931.6 mg (9.22 mmol) of NMA, AIBN, and NBD-OMA was dissolved in methanol. Nitrogen was bubbled through both mixtures for 30 min to remove oxygen. Under vigorous stirring, HEMA was dropped into the flask, and the mixture was placed in an oil bath at a constant temperature of 70 °C for 20 h. The polymerization was quenched through air exposure. A yellow solution was obtained and precipitated in ether to remove unreacted monomers and then dried at a constant temperature of 30 °C. Figures S4, Supporting Information, and 1 show the molecular weight and chemical structure characterization of poly(HEMA-*co*-NMA-*co*-NBD) obtained using GPC with dimethylformamide (DMF) as the eluent and ^{1}H NMR, respectively. The copolymer composition estimated by performing peak integration was consistent with the proposed structure. The copolymer ratio of poly(HEMA-*co*-NMA-*co*-NBD) estimated based on the NMR spectrum is 10.26:1:0.1. Number-averaged molecular weight (M_n) and polydispersity index (PDI) estimated from GPC are 211 913 g mol^{-1} and 1.89, respectively. ^{1}H NMR (DMSO): δ = 8.31 (i), δ = 6.82 (h), δ = 5.48 (d), δ = 4.88 (b), δ = 4.46 (c), δ = 3.88 (a), δ = 3.57 (c), δ = 1.83 (g), δ = 0.83 (f).

Preparation of Electrospun Nanofibers. As shown in Scheme 1b, the ES nanofibers were prepared using a single-capillary spinneret in a procedure similar to that described in our previous report.[25−30] Poly(HEMA-*co*-NMA-*co*-NBD) (200 mg/mL) was dissolved in a methanol (MeOH) solvent and stirred overnight. SRhBOH in concentrations of 0, 1, 5, 10, and 20 wt % (with respect to the poly(HEMA-*co*-NMA-*co*-NBD)) was added to the polymer solution and stirred overnight to fabricate the ES nanofibers. The blended solution was injected into a metallic needle by using syringe pumps (KD Scientific model 100, USA) at a constant rate of 0.5 mL/h. The tip of the metallic needle was connected to a high-voltage power supply (Chargemaster CH30P SIMCO, USA) that was set at 12.9 kV during the ES process. A piece of aluminum foil or quartz was placed 15 cm below the tip of the needle for 30 min to collect the ES nanofibers. All experiments were conducted at room temperature and approximately 60% relative humidity. Poly(HEMA-*co*-NMA-*co*-NBD) blended with ratios of SRhBOH ranging from 0 to 20 wt % are

DOI: 10.1021/am508029x
ACS Appl. Mater. Interfaces 2015, 7, 2797−2808

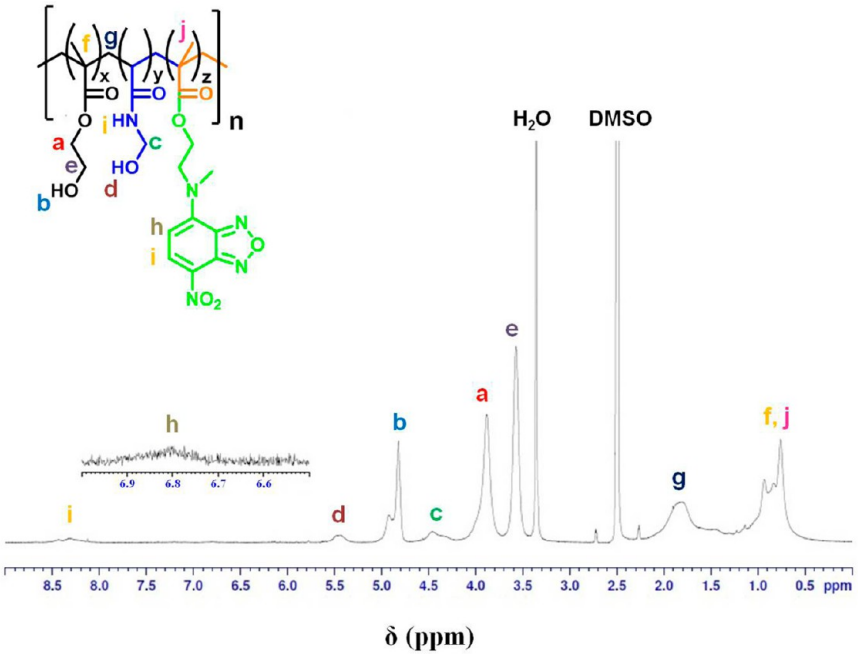

Figure 1. [1]H NMR spectra of poly(HEMA-*co*-NMA-*co*-NBD) in *d*-DMSO.

denoted **P-0%** to **P-20%** (Table 1). The ES nanofibers were annealed at 100 °C for 24 h in an oven for chemical cross-linking.

Table 1. Compositions and CIE Coordinates of FRET-Based ES Nanofibers from poly(HEMA-*co*-NMA-*co*-NBD)/ SRhBOH Blends in Solutions with pH 2, pH 7, or 10^{-3} M Fe^{3+}

ES nanofibers[a]	SRhBOH content	CIE coordinates (in pH = 7)	CIE coordinates (in pH = 2)	CIE coordinates (in 10^{-3} M Fe^{3+})
P-0%	0%	(0.36, 0.62)	(0.36, 0.62)	(0.35, 0.62)
P-1%	1%	(0.36, 0.62)	(0.39, 0.59)	(0.40, 0.58)
P-5%	5%	(0.36, 0.61)	(0.46, 0.52)	(0.47, 0.52)
P-10%	10%	(0.36, 0.61)	(0.53, 0.46)	(0.50, 0.49)
P-20%	20%	(0.36, 0.61)	(0.55, 0.44)	(0.52, 0.47)

[a]ES nanofibers prepared from poly(HEMA-*co*-NMA-*co*-NBD) blending with 0–20% SRhBOH.

Characterization. [1]H NMR data was recorded at room temperature by using a Bruker AM 300 (300 MHz) spectrometer and the residual proton resonance of deuterated chloroform and deuterated dimethyl sulfoxide. ESI-MS spectra were recorded using a Shimadzu LCMS-IT-TOF mass spectrometer. GPC analysis was performed using a Lab Alliance RI2000 instrument (two column, MIXED-C and -D from Polymer Laboratories) connected with one refractive index detector from Schambeck SFD GmbH. All GPC analyses were performed using a polymer/DMF solution at a flow rate of 1 mL/min at 40 °C and calibrated with polystyrene. Fourier transform infrared (FT-IR) spectra were recorded using a Bio-Rad 155 FT-IR spectrometer at ambient temperature in the range of 0–4000 cm^{-1}. The thermal decomposition temperature was determined using a thermal gravimetric analyzer (TGA) from TA Instruments (TGA Q50) in a heating range of 100–800 °C at a heating rate of 10 °C/min in a nitrogen atmosphere.

The morphologies of ES nanofibers were characterized using SEM (Hitachi S-520) and TEM (Hitachi H-600). SEM samples were coated with platinum prior to characterization of the images, and analysis was performed at an acceleration of 15 kV. TEM images were taken using a TEM operated at 100 kV. The SRhBOH domains were selectivity stained with ruthenium tetroxide (RuO_4) and appeared dark, whereas the unstained HEMA/NMA domains appeared light in TEM images. Fluorescence optical microscope images were taken using a two-photon laser confocal microscope (Leica LCS SP5). The morphologies of ES nanofibers were similar to those reported in our previous study.[29]

UV–vis absorption and PL spectra were measured to study photophysical properties. UV–vis absorption spectra were recorded using a Shimadzu UV–vis spectrophotometer. PL experimental data were recorded using a Fluorolog-3 spectrofluorometer (Horiba Jobin Yvon). The variation in the optical absorption and PL of the prepared ES nanofibers (**P-0%** to **P-20%**) with different concentrations of pH and metal ions is described as follows. To ensure that the beam excited the same point on the prepared samples at each measurement, the ES nanofibers were fixed in cuvettes by using an adhesive tape and filled with an aqueous metal ion solution at 10^{-6}–10^{-2} M or acidic and basic aqueous solutions. Each measurement was maintained for 15 min to ensure that an equilibrium of the chelating reaction was reached. All PL spectra of the ES fibers were recorded using the Fluorolog-3 spectrofluorometer and excited at a wavelength of 460 nm, as described in our previous studies.[27,29,30]

RESULTS AND DISCUSSION

Characterization of NBD-OMA, SRhBOH, and Poly-(HEMA-*co*-NMA-*co*-NBD). The chemical structures of NBD-OMA and SRhBOH were characterized using [1]H NMR and ESI-MS, as shown in Figures S1–S3 (Supporting Information). The synthetic routes of NBD-OMA and SRhBOH are shown in Scheme 2 and were similar those previously reported.[20,35–37] Scheme 1a shows the scheme according to which poly(HEMA-*co*-NMA-*co*-NBD) copolymers were synthesized through free radical polymerization. Figure 1 shows the [1]H NMR spectrum of poly(HEMA-*co*-NMA-*co*-NBD), which was composed of HEMA, NMA, and NBD in a ratio of 90.3:8.8:0.9 in DMSO. The proton peak for DMSO is shown in Figure 2. A proton signal of the phenyl group and an aromatic ring on the NBD moiety were observed at 6.8 and 8.3 ppm, respectively (peaks h and i). The proton peaks at 4.8 (peak b) and 3.8 ppm (peak a) represent the terminal hydroxyl moiety and methylene neighbor of oxygen, respectively, on HEMA. The peaks at 5.4 (peak d) and 8.3 ppm (peak i) represent the terminal hydroxyl

DOI: 10.1021/am508029x
ACS Appl. Mater. Interfaces 2015, 7, 2797–2808

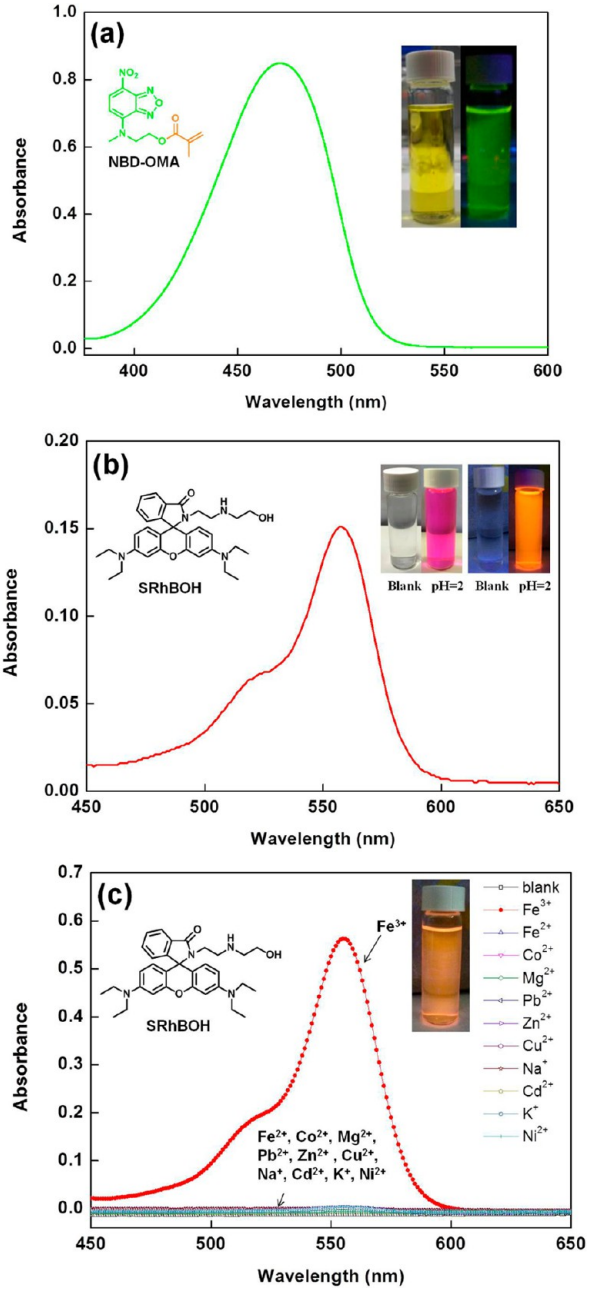

Figure 2. UV−vis spectra of (a) NBD-OMA in CH_3OH solution (4×10^{-5} M) and (b) SRhBOH in CH_3OH solution (10^{-2} M) under pH 2 condition. (c) Variation of UV−vis spectra of SRhBOH in CH_3CN solution (10^{-5} M, pH 7) with different metal ions at 10^{-4} M. Corresponding inset figures show the color changes under visible light and 254 nm UV light.

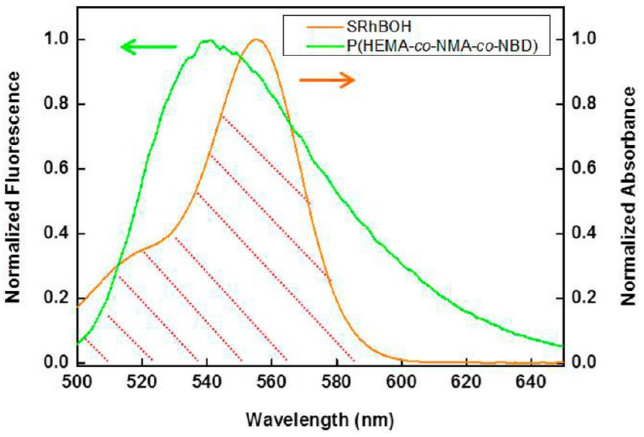

Figure 3. PL spectrum of poly(HEMA-*co*-NMA-*co*-NBD) and UV−vis absorption spectrum of SRhBOH in CH_3OH solution under pH 2 condition.

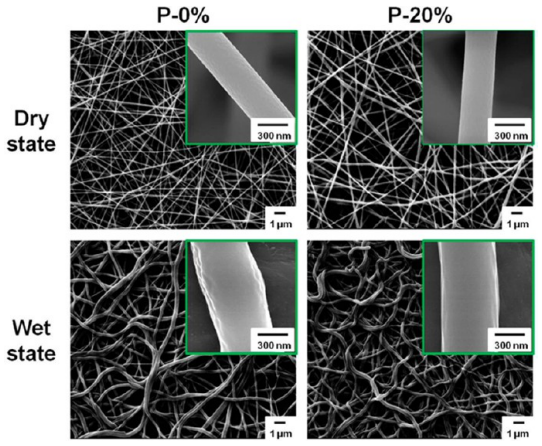

Figure 4. FE-SEM images of the cross-linked **P-0%** and **P-20%** ES nanofibers in the dry state and wet state (treated with water). (Inset) FE-SEM images show an enlarged view of the aforementioned fibers.

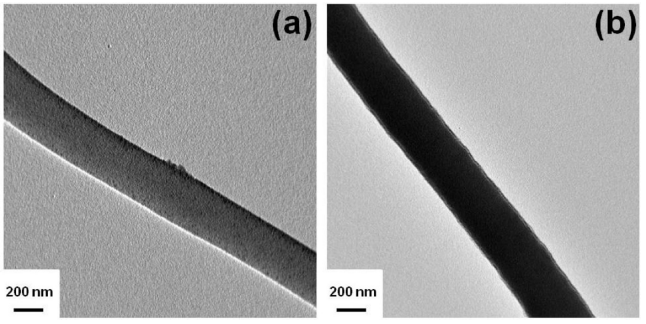

Figure 5. TEM images of **P-20%** ES nanofibers (a) before and (b) after chelating Fe^{3+} ions in aqueous solution (10^{-3} M; pH 7).

moiety and the secondary amine moiety, respectively, on NMA. The peak at 0.8 ppm (peaks f and j) represents the alkyl chains on the polymer. The copolymer composition estimated by performing peak integration was consistent with the proposed structure.

Figure 2a shows that the NBD-OMA in CH_3OH had an absorption peak maximum (λ^{abs}_{max}) of 475 nm and emitted green fluorescence under 254 nm UV light (inset figure). Figure 2b shows the variation in the UV−vis absorption of SRhBOH during pH 2 sensing in a CH_3OH solution. As the pH value changed from 7 to 2, a new λ^{abs}_{max} of 552 nm emerged and the color changed from transparent to orange under 254 nm UV light (insert figure). This indicated that when SRhBOH was used to detect H^+, the spirocyclic form of SRhBOH, which is colorless and nonfluorescent, transformed into the opened cyclic form, which is pink and has a strong orange fluorescence, as shown in Scheme 2c. Figure 2c shows the variations in the UV−vis spectra of SRhBOH in a CH_3CN solution containing various types of metal ion at a concentration of 10^{-5} M (pH 7). Under the initial condition (blank) in which no metal ions were present, the UV−vis spectra of SRhBOH exhibited no absorbed peak. An enhanced absorbed intensity corresponding to a

DOI: 10.1021/am508029x
ACS Appl. Mater. Interfaces 2015, 7, 2797−2808

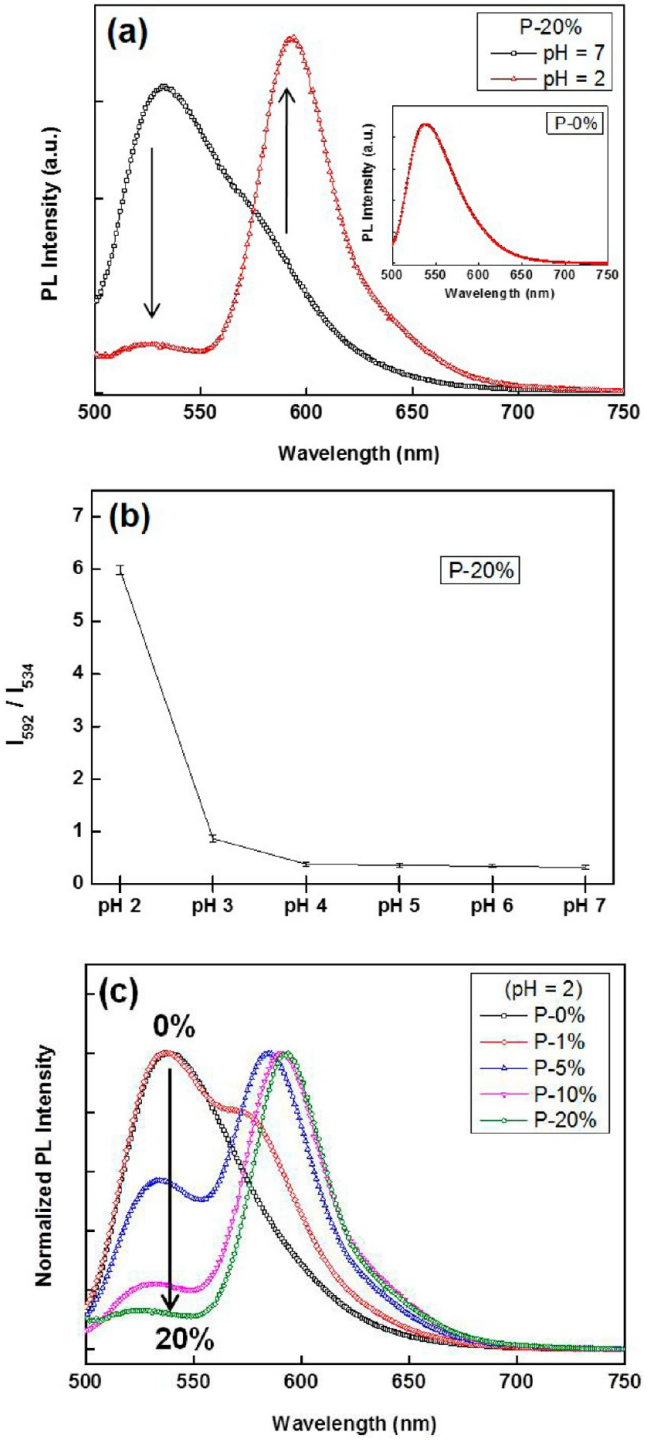

Figure 6. (a) Variation in the PL spectra of **P-20%** ES nanofibers in aqueous solutions with pH 7 and 2. (Inset) PL spectra of **P-0%** ES nanofibers under corresponding conditions. (b) Relative fluorescence intensity changes (I_{592}/I_{534}) of the **P-20%** ES nanofibers in aqueous solution with different pH value. (c) Variation in the normalized PL spectra of **P-0%** to **P-20%** ES nanofibers in aqueous solutions with pH 2.

λ^{abs}_{max} of approximately 552 nm was observed when Fe^{3+} was added. However, no absorbed peak was observed when other metal ions such as Co^{2+}, Mg^{2+}, Na^{+}, Cu^{2+}, Fe^{2+}, Pb^{2+}, Zn^{2+}, Cd^{2+}, K^{+}, and Ni^{2+} were added. This suggested that SRhBOH exhibits high selectivity and sensitivity for Fe^{3+}.

The molecular weights of the poly(HEMA-*co*-NMA-*co*-NBD) copolymer are shown in Figure S4, Supporting Information. The number-average molecular weight (M_n) and polydispersity index (PDI) of poly(HEMA-*co*-NMA-*co*-NBD) were 211 913 and 1.89, respectively. The thermal decomposition curves of the prepared copolymer are shown in Figure S5, Supporting Information. The highest thermal decomposition temperature (T_d) of the copolymer was 317 °C. This indicated that the poly(HEMA-*co*-NMA-*co*-NBD) copolymer exhibited favorable and stable thermal properties.

Figure 3 shows the PL spectrum of poly(HEMA-*co*-NMA-*co*-NBD) and UV−vis absorption spectrum of SRhBOH in CH_3OH solution under pH 2 condition. The PL spectra of poly(HEMA-*co*-NMA-*co*-NBD) subjected to 460 nm excitation had an emission maximum peak (λ^{PL}_{max}) of 540 nm, and the overlapping between the PL spectra of poly(HEMA-*co*-NMA-*co*-NBD) with the optical absorption spectra of SRhBOH (in Fe^{3+} or acidic media) was substantial. Therefore, FRET is efficient and strong when the interchain interaction is high. Thus, the ES nanofibers with different blending ratios of SRhBOH and poly(HEMA-*co*-NMA-*co*-NBD) may exhibit different FRET degrees when they were used to sense different pH values and Fe^{3+} concentrations. This difference in FRET degrees would result in substantial variation in the photophysical properties of ES nanofibers, as discussed in the following sections.

Morphology of Electrospun Nanofibers. Figure 4 shows the FE-SEM images of as-spun ES nanofibers prepared from poly(HEMA-*co*-NMA-*co*-NBD) blended with 0% and 20% SRhBOH (**P-0%** and **P-20%**) in a dry state. These ES nanofibers were cross-linked by annealing them at 100 °C for 24 h. The diameter ranges of the **P-0%** and **P-20%** ES nanofibers were estimated to be 323 ± 42 and 337 ± 38 nm, respectively. The average diameter value was based on the statistical average of 50 fibers from each sample. **P-1%**, **P-5%**, and **P-10%** had the same average fiber diameter of approximately 300 nm, as shown in Figure S6, Supporting Information. The average fiber diameters of the prepared ES nanofibers were similar regardless of the amount of SRhBOH blended into the poly(HEMA-*co*-NMA-*co*-NBD) because of the substantially larger molecular weight of poly(HEMA-*co*-NMA-*co*-NBD) compared with that of SRhBOH. The inset figure shows an enlarged FE-SEM image of the ES nanofibers. All of the ES nanofibers from pure MeOH solvent were smooth and nonporous. In our previous studies[25,38] and another study[39] the rapid evaporation of a low-boiling-point solvent, $CHCl_3$, and a subsequent rapid solidification during the ES process caused the structure of ES nanofibers based on poly(methyl methacrylate) (PMMA) or polystyrene (PS) to be porous. However, although the rapid evaporation of the low-boiling-point solvent MeOH and its subsequent rapid solidification at a high relative humidity (60%) during the ES process may have led to the development of a porous structure, the hydrophilic property of poly(HEMA-*co*-NMA-*co*-NBD) prevented drops from remaining on the surface of solidified as-spun ES nanofibers, possibly causing porous structures to disappear; this is similar to results reported in the literature.[28,30,40]

To observe the morphology of the cross-linked **P-0%** to **P-20%** ES nanofibers after they were used to detect metal ions or H^+ in an aqueous solution, the fibers were collected on a small piece of aluminum foil and immersed in water containing various metal ions or subjected to an acidic condition. After detection, the samples were solidified by placing them into a

DOI: 10.1021/am508029x
ACS Appl. Mater. Interfaces 2015, 7, 2797−2808

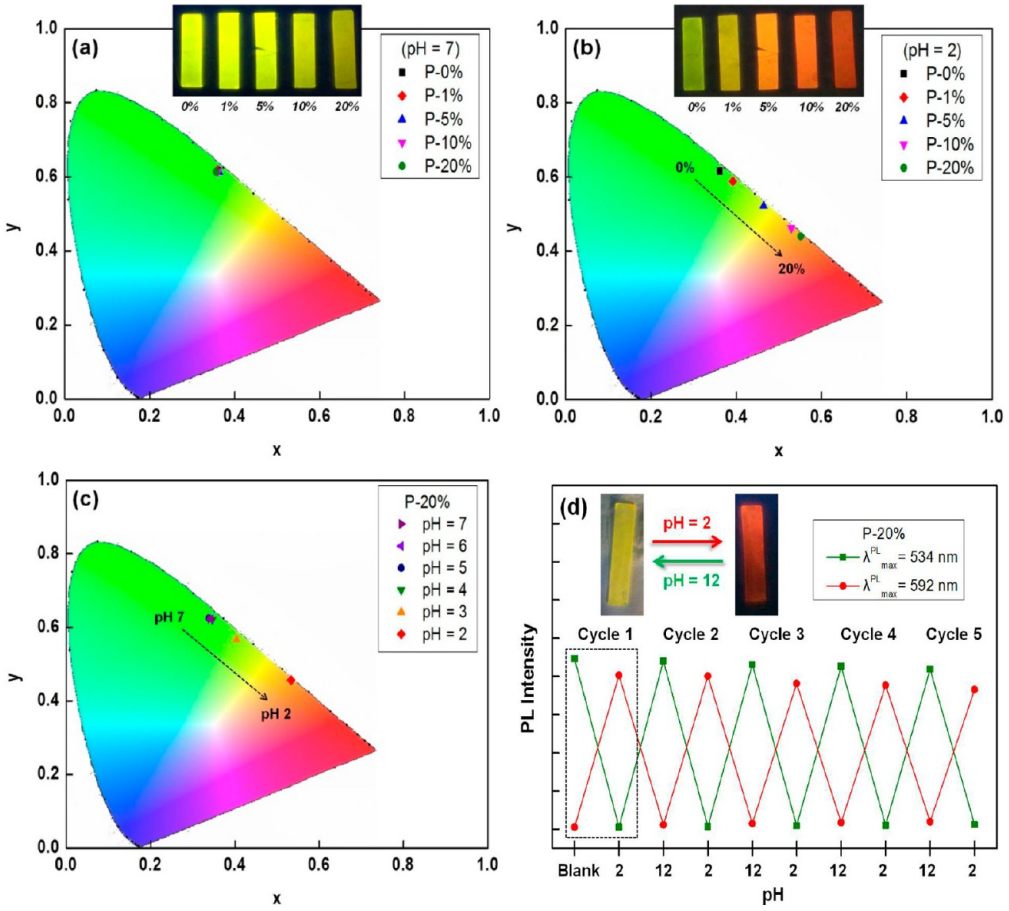

Figure 7. CIE coordinates of **P-0%** to **P-20%** ES nanofibers in aqueous solutions with (a) pH 7 and (b) pH 2. (c) CIE coordinates of **P-0%** to **P-20%** ES nanofibers in aqueous solutions with pH 7 to 2. (d) Reversibility of pH-dependent "on−off−on" fluorescence intensity profile of **P-20%** ES nanofibers. (Insets) Corresponding photographs recorded under UV light.

flask containing liquid nitrogen, and the residual water was removed using a vacuum for 30 min to retain the original morphology. Figure 4 shows FE-SEM images of the wet state of **P-0%** and **P-20%** ES nanofibers after they were used to sense 10^{-3} M Fe^{3+}. The **P-0%** and **P-20%** ES nanofibers were stable in an aqueous solution, as shown in Figure 4 (wet state), exhibiting fiber diameters of 532 ± 152 and 521 ± 167 nm, respectively. The fiber diameter was substantially enlarged after the nanofibers were immersed in water (wet state) compared with that in the dry state (Figure 4; 323 ± 42 and 337 ± 38 nm, respectively) because the hydrophilic HEMA chain swelled in water. However, these swollen fibers maintained their cylindrical shape and did not dissolve in water; this was attributed to the efficient chemical cross-linking of the NMA moiety. Figure S6, Supporting Information, shows the FT-IR spectrum of **P-20%** ES nanofibers annealed at 100 °C for different annealing times, and it shows that the intensity of the −OH peak volume gradually decreased as the annealing time increased, indicating the formation of the intermolecular cross-linking reaction of NMA. These results were similar to those of our previous study.[30] The mechanism of NMA cross-linking is shown in Scheme S1, Supporting Information. The similar swollen fiber morphology and maintained cylindrical shape were also observed in the FE-SEM images of **P-1%**, **P-5%**, and **P-10%** ES nanofibers after the nanofibers were immersed in water (wet state) (Figure S7, Supporting Information).

A TEM image of **P-20%** ES nanofibers before and after they chelated Fe^{3+} is shown in Figure 5a and 5b, respectively. As shown in Figure 5a, the dark dot-like structure with a domain size of 1−5 nm in the TEM image may be attributed to the SRhBOH aggregated domains since it was selectivity stained with RuO_4. The unstained HEMA and NMA domains appeared light in the TEM image. The uniformly dispersed dot-like structure was attributable to the strong stretching force associated with electrospinning, as described in our previous report.[25,41] Furthermore, as shown in Figure 5b, after chelating Fe^{3+}, the **P-20%** ES nanofibers were completely black and substantially darker than before they sensed Fe^{3+}; this was because Fe^{3+} has a high electronic density. This indicated that the **P-20%** ES nanofibers absorbed a substantial amount of Fe^{3+} because of the efficient chelation of the SRhBOH segment. Such chelation between Fe^{3+} and SRhBOH within ES nanofibers resulted in substantial variation in the photophysical properties of ES nanofibers, as discussed in the following sections.

pH-Sensing Property of ES Nanofibers. Figure 6a shows the PL spectra of 20% SRhBOH/poly(HEMA-*co*-NMA-*co*-NBD) blended ES nanofibers (denoted **P-20%**) in acidic (pH 2) and neutral (pH 7) aqueous solutions, and its inset figure shows the corresponding ES nanofibers without SRhBOH (**P-0%**). As shown in the inset figure, the **P-0%** ES nanofibers at either pH 7 or 2 exhibited the same emission maxima (λ^{PL}_{max}) at 534 nm. The λ^{PL}_{max} at 534 nm was attributed to the NBD

DOI: 10.1021/am508029x
ACS Appl. Mater. Interfaces 2015, 7, 2797−2808

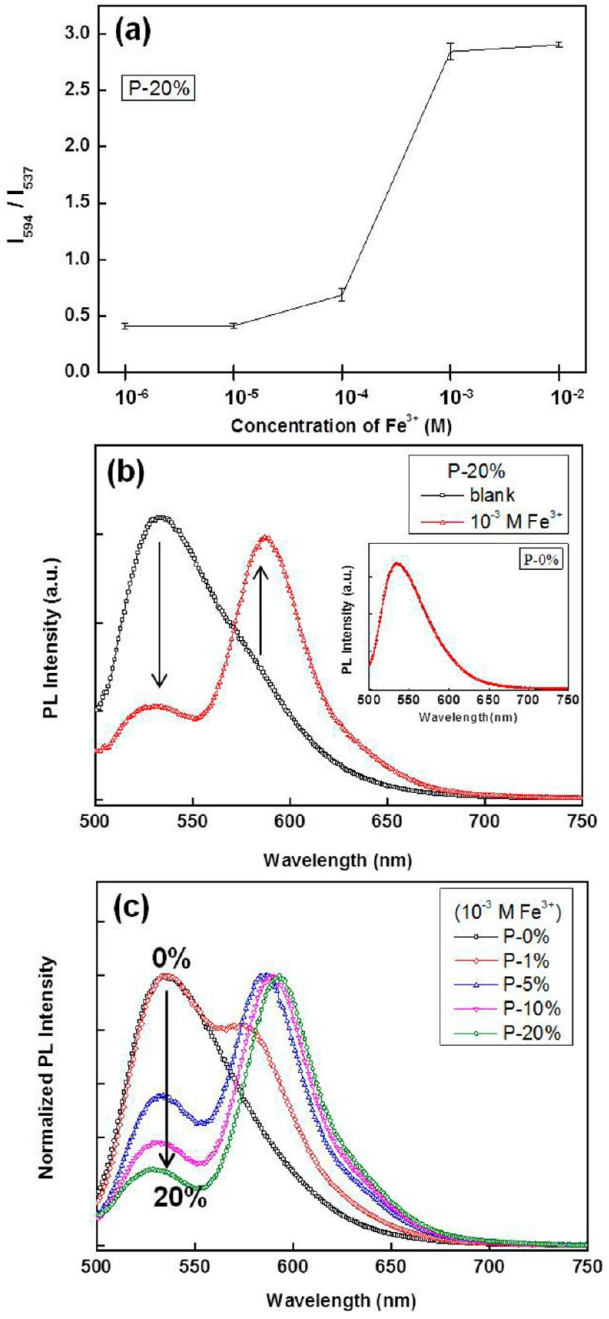

Figure 8. (a) Relative fluorescence intensity changes (I_{594}/I_{537}) of **P-20%** ES nanofibers in aqueous solution with different Fe^{3+} concentrations. (b) Variation in the PL spectra of **P-20%** ES nanofibers in aqueous solutions without Fe^{3+} (blank) and with Fe^{3+} (10^{-3} M). (Inset) PL spectra of **P-0%** ES nanofibers under the aforementioned condition. (c) Variation in the normalized PL spectra of **P-0%** to **P-20%** ES nanofibers in aqueous solutions with Fe^{3+} (10^{-3} M).

moiety under both conditions (pH 7 and 2). However, the **P-20%** ES nanofibers exhibited the λ^{PL}_{max} at 534 (pH 7) and 592 nm (pH 2) (Figure 6a). A marked red shift of λ^{PL}_{max} from 534 to 592 nm was observed as the pH changed from 7 to 2; this shift was caused by the energy transfer between NBD and SRhBOH moieties. While SRhBOH detected H^+, the nonfluorescent spirocyclic form of SRhBOH transformed into the opened cyclic form, which was strongly fluorescent at 592 nm of λ^{PL}_{max}. Hence, such substantial energy transfer can be explained by the overlapping of the emission of poly(HEMA-*co*-NMA-*co*-NBD) and the absorption of SRhBOH in acidic aqueous solution, as shown in Figure 3. A similar energy transfer performance was also observed in the PL spectra of **P-5%** to **P-10%** under acidic condition (Figure S8, Supporting Information).

Figure 6b shows relative fluorescence intensity changes (I_{592}/I_{534}) of the **P-20%** ES nanofibers in aqueous solution with different pH value. It shows the changes of the fluorescence intensity ratio, I_{592}/I_{534} (I_{534} is the fluorescence intensity of NBD emission at 534 nm; I_{592} is the fluorescence intensity of SRhBOH emission at 592 nm), of the **P-20%** ES nanofibers when subjected to H^+. As the pH value was reduced from 7 to 4, I_{592}/I_{534} did not change. However, I_{592}/I_{534} significantly increased from approximately 0.5 to 6.0 as the pH value decreased from 4 to 2; these changes corresponded to the fluorescence of SRhBOH chelated with enough H^+ ions. The **P-20%** ES nanofibers exhibited significant sensing performance in acidic condition starting from pH 4 to 2.

Figure 6c shows normalized PL spectra of **P-0%** to **P-20%** ES nanofibers in an acidic aqueous solution (pH 2). With an increasing ratio of SRhBOH, the NBD emission intensity gradually decreased at approximately 534 nm and the emission peak of SRhBOH substantially increased at approximately 585–592 nm, indicating that energy transfer from NBD to SRhBOH occurred, as described in our previous report.[41] The green emission bands at approximately 534 nm remained in the **P1%** to **P10%** ES nanofibers but completely disappeared in the **P20%** ES nanofibers. This suggested that the increased interchain interaction between NBD and SRhBOH in the ES nanofibers (with 20% SRhBOH blending ratio) led to more efficient energy transfer and shifts in emission spectra.

The Commission Internationale de L'Eclairage (CIE) coordinates[42,43] of the **P-0%** to **P-20%** ES nanofibers in the neutral (pH 7) and acidic (pH 2) aqueous solutions are shown in Figure 7a and 7b, respectively. The corresponding CIE coordinate values are summarized in Table 1. Figure 7a shows that all **P-0%** to **P-20%** ES nanofibers in a neutral aqueous solution (pH 7) with green-light emission had similar CIE coordinates of 0.36 and 0.62. However, a substantial red-shift tendency in the CIE coordinate as the ratio of SRhBOH increased was observed in ES fibers immersed in acidic solution, as shown in Figure 7b. The emission of the **P-0%** to **P-20%** ES nanofibers varied from green (**P-0%**) to green-yellow (**P-1%**), yellow (**P-5%**), orange (**P-10%**), and red (**P-20%**) as the SRhBOH composition increased. This suggested that energy transfer between NBD (donor) and SRhBOH (acceptor) occurred in the fibers, and the different degrees of energy transfer achieved by adjusting the SRhBOH blending ratios yielded various CIE coordinates. A similar trend of a red-shifted CIE coordinate was observed in the **P-20%** ES nanofibers under pH 7 to pH 2 conditions (Figure 7c), indicating that **P-20%** ES nanofibers have a pH-tunable sensing property on fluorescence color changes. Moreover, **P-20%** ES nanofibers exhibited reversible off/on (green/red) switchable fluorescence emission at pH 12 and 2, which can be repeated at least five times, as shown in Figure 7d. At pH 12, **P-20%** ES nanofibers showed green emission (λ^{PL}_{max} at 534 nm) because of the NBD moiety and nonfluorescent spirocyclic SRhBOH. As the pH changed from 12 to 2, the color changed from green to red (λ^{PL}_{max} at 592 nm) because of the energy transfer between the NBD moiety and fluorescent opened cyclic SRhBOH. Finally, the red changed back to green because energy transfer stopped

DOI: 10.1021/am508029x
ACS Appl. Mater. Interfaces 2015, 7, 2797–2808

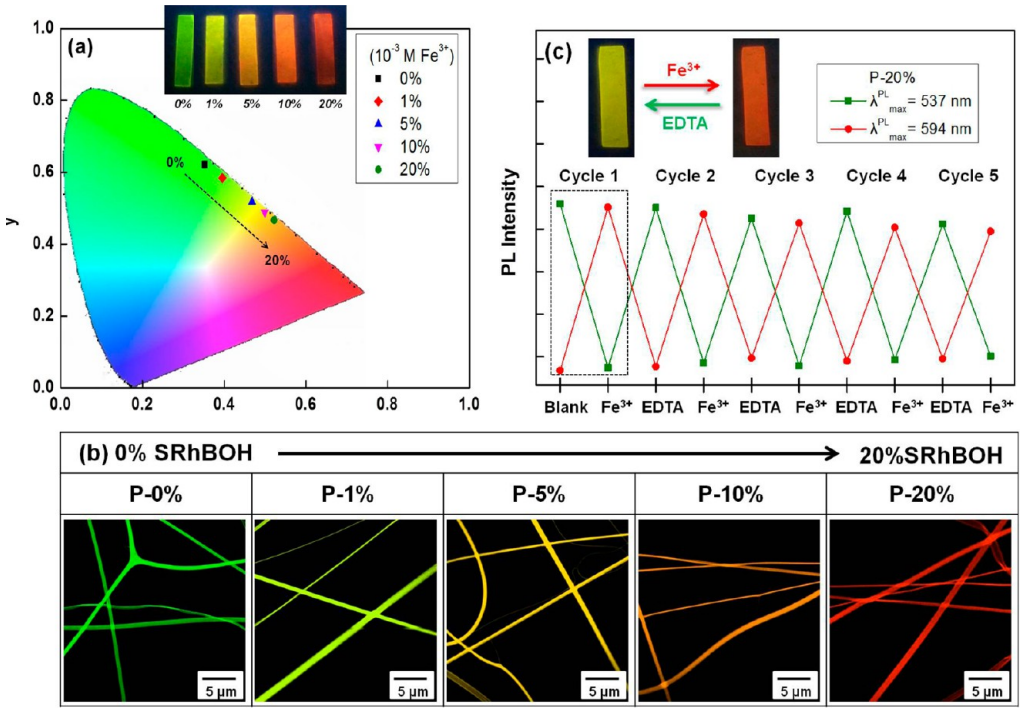

Figure 9. (a) CIE coordinates of **P-0%** to **P-20%** ES nanofibers in aqueous solutions with Fe^{3+} (10^{-3} M). (b) Confocal microscopy images of the ES nanofibers. (c) Reversibility of the Fe^{3+}-dependent "on–off–on" fluorescence intensity profile of **P-20%** ES nanofibers. (Insets) Corresponding photographs recorded under UV light.

when the structure of SRhBOH changed from opened cyclic to spirocyclic. These results revealed that **P-20%** ES nanofibers have excellent pH sensitivity for various pH stimuli and high reversibility.

Fe^{3+}-Sensing Property of ES Nanofibers. SRhBOH is a favorable fluorescent probe for sensing pH and ferric ion (Fe^{3+}). Thus, the capability of SRhBOH/poly(HEMA-*co*-NMA-*co*-NBD) ES nanofibers blended with SRhBOH (**P-0%** to **P-020%**) to sense metal ions was explored. Figure 8a shows the changes of the fluorescence intensity ratio, I_{594}/I_{537} (I_{537} is the fluorescence intensity of NBD emission at 537 nm; I_{594} is the fluorescence intensity of SRhBOH emission at 594 nm), of the **P-20%** ES nanofibers when subjected to Fe^{3+}. As the concentration of Fe^{3+} was increased, NBD (FRET donor) emission at 537 nm gradually decreased and SRhBOH (FRET acceptor) emission at 594 nm increased; these changes corresponded to the fluorescence of SRhBOH chelated with Fe^{3+} ions. It caused I_{594}/I_{537} to increase from approximately 0.5 to 3.0 as the Fe^{3+} ion concentration increased from 10^{-6} to 10^{-2} M. The **P-20%** ES nanofibers exhibited high sensitivity to Fe^{3+} ions at 10^{-4}–10^{-2} M. The binding between SRhBOH and Fe^{3+} ions clearly induced the ring opening of spirolactam rhodomine, which was responsible for the fluorescence intensity ratio changes. The FRET process was activated by Fe^{3+} ion excitation induced by NBD at 460 nm, resulting in fluorescence emission of rhodamine at a maximum of 594 nm. The aforementioned results showed that **P-20%** ES nanofibers are quite sensitive to Fe^{3+} and have a low detection limit of 10^{-4} M. From the titration data of Figure 8a, the dissociation constant (K_d) was calculated as 0.776 mM. In addition, ES nanofibers detected Fe^{3+} in an environment with neutral condition; the selectivity to detect H^+ and Fe^{3+} separately was difficult to achieve when the ES nanofibers were in the environment with both acidic condition and Fe^{3+}. In the environment with both H^+ and Fe^{3+} they exhibited the same performance and color change as they did in the environment with only H^+ or Fe^{3+} (Figure S9, Supporting Information).

Figure 8b shows the PL spectra of **P-20%** ES nanofibers in an aqueous solution without Fe^{3+} (blank) and with Fe^{3+} at 10^{-3} M; its inset figure shows the corresponding spectra of **P-0%** ES nanofibers. The λ^{PL}_{max} of **P-20%** ES nanofibers substantially red shifted from 537 nm in a non-Fe^{3+} aqueous solution to 594 nm in a Fe^{3+} aqueous solution. The large emission maximum shift $\Delta\lambda_{max}$ (57 nm) and luminescence color change from green (537 nm) to red (594 nm) indicated that the nanofibers have high selectivity for Fe^{3+}. However, the **P-0%** ES nanofibers showed no difference in PL regardless of whether the solution contained Fe^{3+}. Figure 8c shows normalized PL spectra of **P-0%** to **P-20%** ES fibers in a Fe^{3+} aqueous solution. As the SRhBOH blending ratio increased, the intensity of λ^{PL}_{max} at 537 nm decreased and $\Delta\lambda_{max}$ increased. This resulted from the stronger energy transfer and interaction between SRhBOH and NBD because using higher SRhBOH blending concentrations results in the chelation of more Fe^{3+}.

Figure 9a shows the CIE coordinates of **P-0%** to **P-20%** ES nanofibers in a 10^{-3} M Fe^{3+} aqueous solution and the corresponding CIE coordinate values are summarized in Table 1. The CIE coordinate red shifted from (0.35, 0.62) (**P-0%**) to (0.47, 0.52) (**P-5%**) and (0.52, 0.47) (**P-20%**) as the SRhBOH content increased. A visible change in fluorescence colors of **P-0%** to **P-20%** ES nanofibers after they were used to chelate Fe^{3+} is shown in the inset image of Figure 9a. Furthermore, as shown in the confocal microscopy images in Figure 9b, the emission colors of the **P-0%** to **P-20%** ES nanofibers varied from green (**P-0%**) to green-yellow (**P-1%**), yellow (**P-5%**), orange (**P-10%**), and red (**P-20%**) as the SRhBOH composition increased. This suggested that an effective switch in the FRET process between NBD (donor)

DOI: 10.1021/am508029x
ACS Appl. Mater. Interfaces 2015, 7, 2797–2808

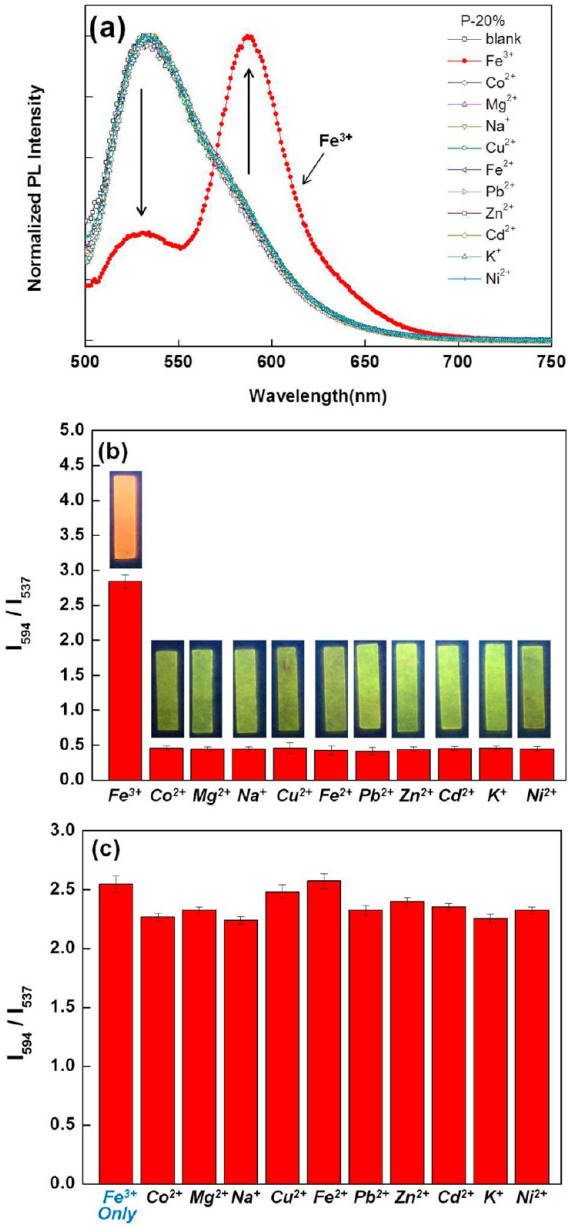

Figure 10. (a) Variation in the normalized PL spectra of **P-20%** ES nanofibers in aqueous solutions with various metal ions (10^{-3} M; pH 7.0) and no cation (blank). (b) Fluorimetric response (I_{594}/I_{537}) of **P-20%** ES nanofibers to various cations at 10^{-3} M in aqueous solutions with pH 7. (From left to right) Fe^{3+}, Co^{2+}, Mg^{2+}, Na^{+}, Cu^{2+}, Fe^{2+}, Pb^{2+}, Zn^{2+}, Cd^{2+}, K^{+}, and Ni^{2+}. (Insets) Corresponding photographs recorded under UV light. (c) Fluorescence enhancement response of **P-20%** ES nanofibers upon addition of metal ions at 10^{-3} M in b followed by addition of Fe^{3+} at 10^{-3} M in aqueous solutions with pH 7.

and ring-opening SRhBOH (acceptor) moieties occurred in the fibers. In addition, the uniform luminescence fibers indicated favorable miscibility between the two components. The **P-20%** ES nanofibers exhibited the strongest interchain interaction and greatest energy transfer with NBD because they had the largest amount of SRhBOH, leading to red emission. As shown in Figure 9c, the red-shifted fluorescence emission (λ^{PL}_{max} at 594 nm) of **P-20%** ES nanofibers can be dramatically enhanced in the presence of Fe^{3+} ions; adding EDTA almost completely restored the emission to the original value obtained in the absence of Fe^{3+}, which was similar to the blank (λ^{PL}_{max} at 537 nm). Moreover, the on/off switchable fluorescence emission of **P-20%** ES nanofibers in aqueous media upon sequential addition of Fe^{3+} and EDTA can be cycled at least five times.

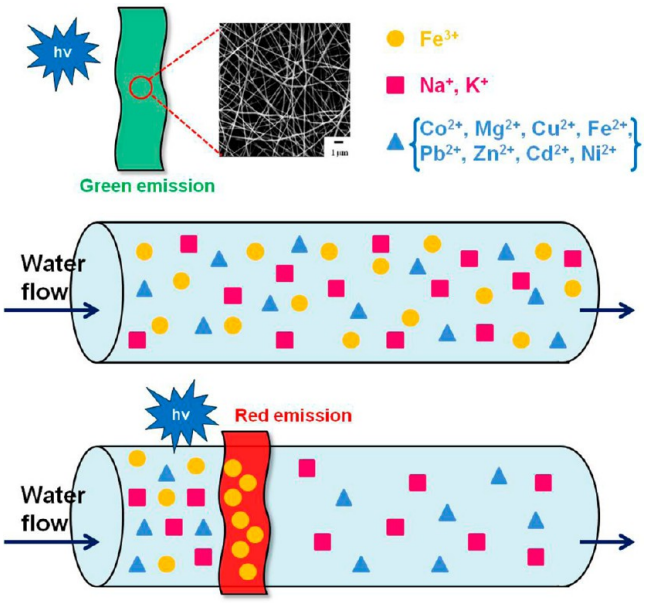

Figure 11. Schematic illustration of a filter-sensory membrane that was prepared from ES nanofibers composed of poly(HEMA-*co*-NMA-*co*-NBD) and SRhBOH blends and chelates and senses Fe^{3+} simultaneously.

The detection selectivity of **P-20%** ES nanofibers toward Fe^{3+} over other common metal ions was also studied (Figure 10). Figure 10a shows that, among all tested metal ions, namely, Co^{2+}, Mg^{2+}, Na^{+}, Cu^{2+}, Fe^{2+}, Pb^{2+}, Zn^{2+}, Cd^{2+}, K^{+}, Ni^{2+}, and Fe^{3+} (10^{-3} M; pH 7), only Fe^{3+} exhibited substantially red-shifted PL. The pH value of the Fe^{3+} or other metal ion test solutions was controlled at 7. The presence of Fe^{3+} induced the most prominent I_{594}/I_{537} enhancement (approximately 2.8-fold), resulting in orange-red emission; all of the other metal ions showed reduced I_{594}/I_{537} values (approximately 0.5-fold), resulting in green emission, as shown in Figure 10b and its inset image. In addition, the fluorescence spectra recorded in the presence of Fe^{3+} ions and the other competing metal ions revealed that all of the other metal ions did not interfere with Fe^{3+}-ion-induced fluorescence enhancement (Figure 10c). This indicated that the sensing of Fe^{3+} by **P-20%** ES nanofibers was almost unaffected by these commonly coexisting ions. In this study, we observed that the **P-20%** ES nanofibers specifically sensed Fe^{3+} (Figure 10b and 10c) and were recoverable and reusable (Figure 9c). Thus, as shown in Figure 11, filter membranes based on the **P-20%** ES nanofibers with a porous architecture specifically chelate with Fe^{3+} in an aqueous solution containing many types of metal ion and have dual-fluorescent chemosensors for Fe^{3+}; these results may assist future researchers in cleaning water while chelating and sensing Fe^{3+} simultaneously. These results indicated that ES nanofibers prepared from SRhBOH/poly(HEMA-*co*-NMA-*co*-NBD) blends have potential for application in multifunctional filter-sensory membrane devices for sensing pH and metal ions.

CONCLUSIONS

New FRET-based dual-ratiometric fluorescent ES nanofibers featuring a multifunctional sensing capability and high sensitivity for pH and Fe^{3+} were prepared using binary blends

DOI: 10.1021/am508029x
ACS Appl. Mater. Interfaces 2015, 7, 2797−2808

of poly(HEMA-*co*-NMA-*co*-NBD)/SRhBOH by employing a single-capillary spinneret. The HEMA, NMA, and NBD moieties were designed to provide hydrophilic properties, chemical cross-linking, and fluorescence (FRET donor), respectively. Cross-linked ES nanofibers maintained their fiber structure in water and sensitivity for pH and Fe^{3+} because of the sufficient NMA composition. The fluorescence emission of SRhBOH (FRET acceptor) within ES nanofibers was highly selective for pH and Fe^{3+} (i.e., nonfluorescent in neutral or alkaline media or an aqueous solution without Fe^{3+} (spirolactam form) and highly fluorescent in acidic media or an aqueous solution with Fe^{3+} (ring-opened acyclic form)). Thus, the off/on switching of FRET can be facilely modulated by adjusting the pH and concentration of Fe^{3+}. In an acidic aqueous solution or Fe^{3+} aqueous solution, the emission of the ES nanofibers varied from green (**P-0%**) to green-yellow (**P-1%**), yellow (**P-5%**), orange (**P-10%**), and red (**P-20%**) as the SRhBOH composition increased. **P-20%** ES nanofibers exhibited the largest $\Delta\lambda_{max}$ of 57 nm, and the luminescence color changed from green to red because of the effective switch in the FRET process between NBD (donor) and ring-opening SRhBOH (acceptor) moieties that occurred in the fibers. Moreover, substantial reversible dual PL between green and red on the **P-20%** ES nanofibers was observed in acidic and alkaline media and in Fe^{3+} and EDTA aqueous solutions. The present study demonstrated that the prepared FRET-based dual-ratiometric fluorescent ES nanofibrous membranes, which can be used as "naked eye" sensors, have potential for application in multifunctional environment sensing devices.

■ ASSOCIATED CONTENT

Supporting Information

Potential cross-linking for NMA−NMA and NMA−hydroxyl cross-links; ^{1}H NMR spectrum of NBD-OMA in $CDCl_3$; ^{1}H NMR spectrum of SRhBOH in $CDCl_3$; ESI-MS spectrum of SRhBOH; GPC curve of poly(HEMA-*co*-NMA-*co*-NBD); TGA curve of poly(HEMA-*co*-NMA-*co*-NBD) at a heating rate of 10 °C/min in a nitrogen atmosphere; IR spectrum of poly-(HEMA-*co*-NMA-*co*-NBD) before and after cross-linking; SEM images of the cross-linked **P-1%**, **P-5%**, and **P-10%** ES nanofibers in the dry state and wet state (treated with water); variation in the PL spectra of **P-1%**, **P-5%**, and **P-10%** ES nanofibers in aqueous solutions with pH 7 and 2; variation in colors of photographs of **P-20%** ES nanofibers in aqueous solutions with Fe^{3+} and pH 2, separately or combined. This material is available free of charge via the Internet at http://pubs.acs.org.

■ AUTHOR INFORMATION

Corresponding Author

*Tel.: 886-2-27712171 (ext 2407). Fax: 886-2-27317174. E-mail: kuocc@mail.ntut.edu.tw.

Notes

The authors declare no competing financial interest.

■ ACKNOWLEDGMENTS

Financial support from the Ministry of Science and Technology of Taiwan (MOST 103-2221-E-027-128) is highly appreciated.

■ REFERENCES

(1) Rurack, K.; Resch-Genger, U. Rigidization, Preorientation and Electronic Decoupling—the 'Magic Triangle' for the Design of Highly Efficient Fluorescent Sensors and Switches. *Chem. Soc. Rev.* **2002**, *31*, 116−127.

(2) Amendola, V.; Fabbrizzi, L.; Foti, F.; Licchelli, M.; Mangano, C.; Pallavicini, P.; Poggi, A.; Sacchi, D.; Taglietti, A. Light-Emitting Molecular Devices Based on Transition Metals. *Coord. Chem. Rev.* **2006**, *250*, 273−299.

(3) Yang, Y. K.; Yook, K. J.; Tae, J. A Rhodamine-Based Fluorescent and Colorimetric Chemodosimeter for the Rapid Detection of Hg^{2+} Ions in Aqueous Media. *J. Am. Chem. Soc.* **2005**, *127*, 16760−16761.

(4) Mao, J.; Wang, L.; Dou, W.; Tang, X.; Yan, Y.; Liu, W. Tuning the Selectivity of Two Chemosensors to Fe(III) and Cr(III). *Org. Lett.* **2007**, *9*, 4567−4570.

(5) Tang, L.; Li, Y.; Nandhakumar, R.; Qian, J. An Unprecedented Rhodamine-Based Fluorescent and Colorimetric Chemosensor for Fe^{3+} in Aqueous Media. *Monatsh. Chem.* **2010**, *141*, 615−620.

(6) Aisen, P.; Marianne, W. R.; Leibold, E. A. Iron Metabolism. *Curr. Opin. Chem. Biol.* **1999**, *3*, 200−206.

(7) Touati, D. Iron and Oxidative Stress in Bacteria. *Arch. Biochem. Biophys.* **2000**, *373*, 1−6.

(8) M. Campbell, L.; Dixon, D. G.; Hecky, R. E. A Review of Mercury in Lake Victoria, East Africa: Implications for Human and Ecosystem Health. *J. Toxicol. Environ. Health, Part B* **2003**, *6*, 325−356.

(9) Lowell, B. B.; Spiegelman, B. M. Towards a Molecular Understanding of Adaptive Thermogenesis. *Nature* **2000**, *404*, 652−660.

(10) Shi, X. L.; Mao, G. J.; Zhang, X. B.; Liu, H. W.; Gong, Y. J.; Wu, Y. X.; Zhou, L. Y.; Zhang, J.; Tan, W. Rhodamine-Based Fluorescent Probe for Direct Bio-Imaging of Lysosomal pH Changes. *Talanta* **2014**, *130*, 356−362.

(11) Liu, A.; Hong, M.; Yang, W.; Lu, S.; Xu, D. One-Pot Synthesis of a New Rhodamine-Based Dually-Responsive pH Sensor and Its Application to Bioimaging. *Tetrahedron* **2014**, *70*, 6974−6979.

(12) Hu, Z. Q.; Li, M.; Liu, M. D.; Zhuang, W. M.; Li, G. K. A Highly Sensitive Fluorescent Acidic pH Probe Based on Rhodamine B Diethyl-2-aminobutenedioate Conjugate and Its Application in Living Cells. *Dyes Pigm.* **2013**, *96*, 71−75.

(13) Fan, J.; Lin, C.; Li, H.; Zhan, P.; Wang, J.; Cui, S.; Hu, M.; Cheng, G.; Peng, X. A Ratiometric Lysosomal pH Chemosensor Based on Fluorescence Resonance Energy Transfer. *Dyes Pigm.* **2013**, *99*, 620−626.

(14) Weerasinghe, A. J.; Schmiesing, C.; Sinn, E. Highly Sensitive and Selective Reversible Sensor for the Detection of Cr^{3+}. *Tetrahedron Lett.* **2009**, *50*, 6407−6410.

(15) Wang, J.; Li, H.; Long, L.; Xiao, G.; Xie, D. Fast Responsive Fluorescence Turn-On Sensor for Cu^{2+} and its Application in Live Cell Imaging. *J. Lumin.* **2012**, *132*, 2456−2461.

(16) Hu, Z. Q.; Lin, C. S.; Wang, X. M.; Ding, L.; Cui, C. L.; Liu, S. F.; Lu, H. Y. Highly Sensitive and Selective Turn-On Fluorescent Chemosensor for Pb^{2+} and Hg^{2+} Based on a Rhodamine-Phenylurea Conjugate. *Chem. Commun.* **2010**, *46*, 3765−3767.

(17) Chen, J.; Zeng, F.; Wu, S.; Su, J.; Tong, Z. Photoreversible Fluorescent Modulation of Nanoparticles via One-Step Miniemulsion Polymerization. *Small* **2009**, *5*, 970−978.

(18) Xu, M.; Wu, S.; Zeng, F.; Yu, C. Cyclodextrin Supramolecular Complex as a Water-Soluble Ratiometric Sensor for Ferric Ion Sensing. *Langmuir* **2010**, *26*, 4529−4534.

(19) Li, C.; Liu, S. Polymeric Assemblies and Nanoparticles with Stimuli-Responsive Fluorescence Emission Characteristics. *Chem. Commun.* **2012**, *48*, 3262−3278.

(20) Ma, B.; Wu, S.; Zeng, F.; Luo, Y.; Zhao, J.; Tong, Z. Nanosized Diblock Copolymer Micelles as a Scaffold for Constructing a Ratiometric Fluorescent Sensor for Metal Ion Detection in Aqueous Media. *Nanotechnology* **2010**, *21*, 195501.

(21) Wan, X.; Liu, S. Fluorescent Water-Soluble Responsive Polymers Site-Specifically Labeled with FRET Dyes Possessing pH- and Thermo-Modulated Multicolor Fluorescence Emissions as Dual Ratiometric Probes. *J. Mater. Chem.* **2011**, *21*, 10321−10329.

DOI: 10.1021/am508029x
ACS Appl. Mater. Interfaces 2015, 7, 2797−2808

(22) H Reneker, D.; Chun, I. Nanometre Diameter Fibres of Polymer, Produced by Electrospinning. *Nanotechnology* **1996**, *7*, 216−223.
(23) Babel, A.; Li, D.; Xia, Y.; Jenekhe, S. A. Electrospun Nanofibers of Blends of Conjugated Polymers: Morphology, Optical Properties, and Field-Effect Transistors. *Macromolecules* **2005**, *38*, 4705−4711.
(24) Chae, S. K.; Park, H.; Yoon, J.; Lee, C. H.; Ahn, D. J.; Kim, J. M. Polydiacetylene Supramolecules in Electrospun Microfibers: Fabrication, Micropatterning, and Sensor Applications. *Adv. Mater.* **2007**, *19*, 521−524.
(25) Kuo, C. C.; Lin, C. H.; Chen, W. C. Morphology and Photophysical Properties of Light-Emitting Electrospun Nanofibers Prepared from Poly(fluorene) Derivative/PMMA Blends. *Macromolecules* **2007**, *40*, 6959−6966.
(26) Huang, Y. S.; Kuo, C. C.; Shu, Y. C.; Jang, S. C.; Tsen, W. C.; Chuang, F. S.; Chen, C. C. Highly Aligned and Single-Layered Hollow Fibrous Membranes Prepared from Polyurethane and Silica Blends Through a Two-Fluid Coaxial Electrospun Process. *Macromol. Chem. Phys.* **2014**, *215*, 879−887.
(27) Kuo, C. C.; Tung, Y. C.; Chen, W. C. Morphology and pH Sensing Characteristics of New Luminescent Electrospun Fibers Prepared from Poly(phenylquinoline)-*block*-Polystyrene/Polystyrene Blends. *Macromol. Rapid Commun.* **2010**, *31*, 65−70.
(28) Chiu, Y. C.; Kuo, C. C.; Hsu, J. C.; Chen, W. C. Thermoresponsive Luminescent Electrospun Fibers Prepared From Poly(DMAEMA-*co*-SA-*co*-StFl) Multifunctional Random Copolymers. *ACS Appl. Mater. Interfaces* **2010**, *2*, 3340−3347.
(29) Chiu, Y. C.; Chen, Y.; Kuo, C. C.; Tung, S. H.; Kakuchi, T.; Chen, W. C. Synthesis, Morphology, and Sensory Applications of Multifunctional Rod−Coil−Coil Triblock Copolymers and Their Electrospun Nanofibers. *ACS Appl. Mater. Interfaces* **2012**, *4*, 3387−3395.
(30) Chen, L. N.; Chiu, Y. C.; Hung, J. J.; Kuo, C. C.; Chen, W. C. Multifunctional Electrospun Nanofibers Prepared from Poly((N-isopropylacrylamide)-*co*-(N-hydroxymethylacrylamide)) and Their Blends with 1,2-Diaminoanthraquinone for NO Gas Detection. *Macromol. Chem. Phys.* **2014**, *215*, 286−294.
(31) Wang, X.; Drew, C.; Lee, S. H.; Senecal, K. J.; Kumar, J.; Samuelson, L. A. Electrospun Nanofibrous Membranes for Highly Sensitive Optical Sensors. *Nano Lett.* **2002**, *2*, 1273−1275.
(32) Wang, W.; Yang, Q.; Sun, L.; Wang, H.; Zhang, C.; Fei, X.; Sun, M.; Li, Y. Preparation of Fluorescent Nanofibrous Film as a Sensing Material and Adsorbent for Cu^{2+} in Aqueous Solution via Copolymerization and Electrospinning. *J. Hazard. Mater.* **2011**, *194*, 185−192.
(33) Syu, J. H.; Cheng, Y. K.; Hong, W. Y.; Wang, H. P.; Lin, Y. C.; Meng, H. F.; Zan, H. W.; Horng, S. F.; Chang, G. F.; Hung, C. H.; Chiu, Y. C.; Chen, W. C.; Tsai, M. J.; Cheng, H. Electrospun Fibers as a Solid-State Real-Time Zinc Ion Sensor with High Sensitivity and Cell Medium Compatibility. *Adv. Funct. Mater.* **2013**, *23*, 1566−1574.
(34) Chen, X.; Pradhan, T.; Wang, F.; Kim, J. S.; Yoon, J. Fluorescent Chemosensors Based on Spiroring-Opening of Xanthenes and Related Derivatives. *Chem. Rev.* **2012**, *112*, 1910−1956.
(35) Alonso, A.; Catalina, F.; Salvador, E. F.; Peinado, C. Synthesis of Amphiphilic Random Copolymers and Fluorescence Study of Their Association Behavior in Water. *Macromol. Chem. Phys.* **2001**, *202*, 2293−2299.
(36) Bosma, G.; Pathmamanoharan, C.; de Hoog, E. H. A.; Kegel, W. K.; Blaaderen, A. v.; Lekkerkerker, H. N. W. Preparation of Monodisperse, Fluorescent PMMA−Latex Colloids by Dispersion Polymerization. *J. Colloid Interface Sci.* **2002**, *245*, 292−300.
(37) Kalinina, O.; Kumacheva, E. A "Core-Shell" Approach to Producing 3D Polymer Nanocomposites. *Macromolecules* **1999**, *32*, 4122−4129.
(38) Chen, H. C.; Wang, C. T.; Liu, C. L.; Liu, Y. C.; Chen, W. C. Full Color Light-Emitting Electrospun Nanofibers Prepared from PFO/MEH-PPV/PMMA Ternary Blends. *J. Polym. Sci., Part B: Polym. Phys.* **2009**, *47*, 463−470.
(39) Kwak, G.; Fukao, S.; Fujiki, M.; Sakaguchi, T.; Masuda, T. Nanoporous, Honeycomb-Structured Network Fibers Spun from Semiflexible, Ultrahigh Molecular Weight, Disubstituted Aromatic Polyacetylenes: Superhierarchical Structure and Unique Optical Anisotropy. *Chem. Mater.* **2006**, *18*, 5537−5542.
(40) Chen, L. N.; Kuo, C. C.; Chiu, Y. C.; Chen, W. C. Ultra Metal Ions and pH Sensing Characteristics of Thermoresponsive Luminescent Electrospun Nanofibers Prepared from Poly(HPBO-*co*-NIPAAm-*co*-SA). *RSC Adv.* **2014**, *4*, 45345−45353.
(41) Wang, C. T.; Kuo, C. C.; Chen, H. C.; Chen, W. C. Non-Woven and Aligned Electrospun Multicomponent Luminescent Polymer Nanofibers: Effects of Aggregated Morphology on the Photophysical Properties. *Nanotechnology* **2009**, *20*, 375604.
(42) Smith, T.; Guild, J. The C.I.E. Colorimetric Standards and Their Use. *Trans. Opt. Soc.* **1931**, *33*, 73−134.
(43) Poynton, C. *A Guided Tour of Color Space*; John Wiley & Sons: New York, 1997; pp 1−14.

DOI: 10.1021/am508029x
ACS Appl. Mater. Interfaces 2015, 7, 2797−2808